Available online at www.sciencedirect.com

ScienceDirect

Green Energy & Environment 1 (2016) 246–257

www.keaipublishing.com/gee

Research paper

Thermodynamic modelling of unloaded and loaded N,N-diethylethanolamine solutions

Monica Garcia [a,*], Hanna K. Knuutila [b], Sai Gu [a]

[a] Department of Chemical and Process Engineering, Faculty of Engineering and Physical Sciences, University of Surrey, Guildford, Surrey, GU2 7XH, UK
[b] Department of Chemical Engineering, Norwegian University of Science and Technology (NTNU), Sem Saeland Vei 4, Trondheim, NO-7045, Norway

Received 4 September 2016; revised 10 November 2016; accepted 11 November 2016
Available online 25 November 2016

Abstract

Chemical absorption is a crucial step for several chemical processes such as ammonia production, coal gasification, methane reforming, ethylene oxide manufacturing and treatment of associated gas streams [1]. It is considered one of the main processes to eliminate CO_2 emissions from power plants by post-combustion.

Use of new solvents are of high interest in chemical absorption for carbon capture. For the design of the absorption and desorption columns it is essential to know the vapour–liquid equilibrium (VLE), heat of absorption and densities. N,N-diethylethanolamine (DEEA) appeared as one of the amines with the lowest amount of energy needed for its regeneration [2], which would directly decrease the operation costs. DEEA has a high CO_2 loading of 1 mol/mol of amine compared to the traditional MEA solvent (0.5 mol/mol amine) and is obtained from renewable sources [1]. The main weakness is its low absorption rate and consequently the use of promoters is desirable.

In this work, a thermodynamic model based on the electrolyte non-random two-liquid theory (eNRTL) was created and fitted to correlate and predict the partial and total pressures of the unloaded and loaded aqueous DEEA solutions. New interaction parameters were obtained for the binary and tertiary system. This model represents the vapour pressures of the pure components, DEEA and H_2O, with AARD of 1.9% and 1.73% respectively. Furthermore, the fitted model predicts the total pressure above the binary system, H_2O-DEEA, with AARD of 0.05%. The excess of enthalpy and densities are predicted with AARD of 5.63% and 1.38% respectively. The tertiary system, H_2O-DEEA-CO_2, is fitted for 2 M and 5 M DEEA solutions with loading between 0.042 and 0.9 mol CO_2/mol amine up to 80 °C. Results of CO_2 partial pressures and total pressures are reproduced, with AARD of 19.45% and 16.18% respectively. Densities are predicted with an AARD of 1.52%.

Keywords: DEEA; CO_2 capture; Chemical absorption; Modelling

1. Introduction

Carbon capture has been recognised as the only way to reach the world-wide compromise for climate change, which is the target of 2 °C over the Earth's temperature registered in 1990 [3]. Moreover, the European Commission supported this point of view in 2014 [4]. In this context, chemical absorption technology offers benefits in the refurbishment of traditional plants and is a proven industrial scale agent for the removal of other acid gases. However, in terms of carbon capture, this technology still needs to be optimized for better economic and efficiency performance. Stakeholders consider that the use of new solvents is essential for the maturity of post-combustion systems and its market competitiveness [5–7].

Amines are commonly used for carbon capture. Primary and secondary amines are known for its capacity to form carbamates when reacting with CO_2. This step has a high kinetic rate that makes them desirable to use in carbon capture. However, the energy required for regeneration is high. In contrast, tertiary

* Corresponding author.
E-mail address: m.garcia@surrey.ac.uk (M. Garcia).

http://dx.doi.org/10.1016/j.gee.2016.11.003

Table 1
Sets of parameters used for fitting and validation of the simulation model presented in this work.

Data	[DEEA]	Temperature (°C)	Loading (mol CO_2/mol DEEA)	Points	References
CO_2 Partial pressure	2 M	40, 60, 80	0.02–0.888	43	[20]
CO_2 Partial Pressure	5 M	40, 60, 80	0.005–0.398	42	[20]
Total Pressure	2 M	80	0.71–1.02	9	[20]
Total Pressure	5 M	80	0.25–0.67	9	[20]
Heat of mixing	0.0472–0.9011 (Molar Fraction)	25	0	18	[23]
Total Pressure	5 M	40	0.039–1.038	44	[24]
CO_2 Partial Pressure	5M	40, 80	0.038–0.990	68	[24]
Density	0–1 (Molar Fraction)	20–70	0	106	[25]
Density	2 M	20–70	0.14–0.79	36	[25]
Density	5 M	20–70	0.14–0.42	20	[25]
Density	0-1 (Molar Fraction)	20–40	0	96	[29]
Density	0–1 (Molar Fraction)	25–45	0	78	[28]
Vapour pressure	1	5–45	0	31	[20]
Vapour pressure	1	60–176	0	13	[30]
Vapour pressure	0.0015–0.5611 (Molar Fraction)	50–95	0	44	[15]
Water vapour pressure	0	49–144	0	7	[26]
Water vapour pressure	0	34–100	0	50	[27]

amines require less heat for stripping but have a much slower reaction rate. Solvent vaporization, corrosion, toxicity and environmental issues are other aspects to take into account for the selection of the solvent. Over the years, an extensive number of single alkanolamines and proprietary formulations have been proposed [8–11]. N,N-diethylethanolamine (DEEA) has been presented as a new candidate to use for the removal of CO_2 [10,12–15]. This tertiary amine is the result of the reaction of ethylene oxide and diethylamine. Ethanol, the main raw material used to produce DEEA, can be obtained from natural sources and, consequently, this amine is considered a renewable solvent [1]. DEEA has a high CO_2 loading of 1 mol/mol of amine in comparison to the traditional MEA solvent (0.5 mol/mol amine). However, as the kinetic rate is lower than primary amines, it is desirable to use a promoter. Several authors have studied the blends made by DEEA and primary amines. Kim & Svendsen [2] included in their work the heat of absorption of several pure solvents and their blends. In their comparison, DEEA and MDEA appeared as the amines with the lowest energy needed for its regeneration. Also Arshad et al. [16] included in their work the heat of absorption of DEEA, MAPA and its blend with water. They concluded that, in comparison to MAPA, the tertiary amine has a lower heat of absorption, which depends only on temperature. For the blends, the heat of absorption depends also on the CO_2 loading and amines composition.

This heat of absorption impacts directly on operation costs. Broeder & Svendsen [17] studied potential solvents, including blends of DEEA with primary amines. Conway et al. [18] included in their work 4 M and 3 M DEEA solutions promoted with MEA. In their results, the kinetic rate increased as the MEA content increases, while cyclic capacity was optimum at lower MEA concentration. Hartono et al. [15] incorporated in their work pure DEEA and its mixture with MAPA and water, while Konduru et al. [13] studied DEEA activated with PZ (piperazine). In addition, Vaidya and Kenig [1] included the blend of DEEA+Ethylethanolamine (EEA) and DEEA+PZ.

Simulation of DEEA can be crucial for the design and prediction of the chemical absorption. Specifically, knowing the VLE is essential for the design of absorber and desorber columns [19]. Monteiro et al. [20] studied the system DEEA-H_2O-CO_2 using an in-house-VLE model using the eNRTL-model to calculate the activities in the liquid phase. The model was fitted to experimental data, which included the VLE and heat of absorption of the systems DEEA+H_2O and DEEA+CO_2+H_2O. The developed model represented the experimental data well, with AARD below 18%. Moreover, the study presented new data for physical solubility, Antoine's parameters for vapour pressures, equilibrium constant of DEEA and interaction parameters. However, this work was based on an in-house-VLE model that predicted the interaction parameters. Using these optimised parameters in Aspen Plus v8.6 does not give a good fit of experimental data. This absent of fitting indicates that there are some differences in the implementation of the vapour–liquid equilibrium model using the eNRTL model, in-house and in Aspen Plus.

Xu et al. [21] modelled the systems DEEA-H_2O and DEEA-H_2O-CO_2 with Aspen Plus and reported the parameters

Table 2
Pure physical properties of DEEA, H_2O and CO_2 [31].

	DEEA	H_2O	CO_2
P_C (kPa)	3180	7374	22060
T_C (K)	592	304.13	647.3
V_C cum/kmol	0.401	0.0939	0.0559
Zc	0.259	0.274	0.229
Acentric factor	0.782	0.225	0.344

Table 3
Dielectric constants, where T_{ref} has been set at 298.15 K [32].

$$\varepsilon(T) = a + b\left(\frac{1}{T} - \frac{1}{T_{ref}}\right)$$

	H_2O	DEEA
a	2.6227	78.65
b	54.501	31989

Table 4
Equilibrium constants used in this work for R1-R4.

$lnK_{eq} = A + \frac{B}{T} + ClnT + DT$

Reaction	A	B	C	D	Source
1	132.8	−13445.9	−22.3773	0	[36]
2	232	−12092.1	−36.7816	0	[36]
3	216.049	−12431.7	−35.4819	0	[36]
4	−110	90.5882	14.5518	0.0028	This work

Table 5
Description of contributions to the excess free Gibbs energy [35].

$G^E = G^{E,PDH} + G^{E,Born} + G^{E,lc}$

Term	Expression
$G^{E,PDH}$	$-RT(\sum_k x_k)\left(\frac{1000}{M_s}\right)^{0.5}\left(\frac{4A_\phi I_x}{\rho}\right) ln(1+\rho I_x^{0.5})$
$G^{E,Born}$	$RT\left(\frac{e^2}{2kT}\right)\left(\frac{1}{\varepsilon_s}-\frac{1}{\varepsilon_w}\right)\left(\sum_i \frac{x_i z_i^2}{r_i}\right)10^{-2}$
$G^{E,lc}$	$\sum_m x_m \frac{\sum_j x_j \tau_{jm} G_{jm}}{\sum_k x_k G_{jm}} + \sum_c x_c \sum_{a'}\left(\frac{x_{a'}}{\sum_{a''} x_{a''}}\right)\left(\frac{\sum_j \tau_{jc,a'c} G_{jc}}{\sum_k x_k G_{kc,a'c}}\right) + \ldots$ $+ \sum_z x_a \sum_{c'}\left(\frac{x_{c'}}{\sum_{c''} x_{c''}}\right)\left(\frac{\sum_j \tau_{ja,a'c} G_{ja}}{\sum_k x_k G_{kc,a'c}}\right)$

used. One weakness of their model was that it was fitted with the VLE data of 3 M and 4 M solutions only at 60 and 80 °C. The heat of absorption was represented from 40 to 120 °C for loaded 1 M and 4 M DEEA solutions, and at 60 and 80 °C for loaded 3 M DEEA solutions. In addition, Xu et al. [21] did not discuss the accuracies of their model. From the graphs reported, the simulation model seems to have qualitatively large differences between experimental and simulation results. The loading range validated was limited (0.4–0.8 and 0.2–0.5 mol CO_2/mol amine for 3 M and 4 M DEEA solutions respectively). VLE and heat of absorption of unloaded solutions were fitted to data from Touhara et al. [22] and Mathonat et al. [23]. Although errors were not reported, the qualitative differences with Mathonat et al. [23] seem to be high. However, it is unclear what data was used from Touhara et al. [22], since no DEEA data is found in that paper.

Arshad et al. [24] used VLE and heat of absorption data to model the DEEA-H_2O and DEEA-H_2O-CO_2 systems with the Uniquac framework. To optimize the parameters, they used a mathematical estimation. The parameters were fitted for 5 M and 2 M DEEA solutions. The AARD obtained in their work was 11% for the pressure and 7% for the excess of enthalpy of the binary system. This model reported AARD of 9.55% and 17.4% for the total and partial pressures of the tertiary system repectively. In this work, it was not reported the Antoine's equation or kinetics parameters and densities were not considered.

In addition to the reports commented above, Pinto et al. [25] reported several density models fitted to experimental data of the binary and tertiary systems, DEEA-H_2O and DEEA-H_2O-CO_2. Their model covered a wide range of temperatures, from 20 to 70 °C, with loadings from 0 to 0.8 mol CO_2/mol DEEA, for aqueous 2 M and 5 M DEEA solutions. They compared the Racket and Redlich-Kister models for unloaded DEEA solutions. Additionally, they included one proportional model for loaded solutions, added to the value of unloaded solutions. The AARD reported were less than 0.1% and 1% approximately for unloaded solutions using Redlich-Kister and Racket models respectively. For the loaded solutions, the AARD was 3.3% and 19.2% using the proportional and Racket models correspondingly. Unfortunately, Redlich-Kister and proportional models are not available in Aspen Plus.

The present work attempts to fill the gap evident from the previous reports on the systems DEEA-H_2O and DEEA-H_2O-CO_2. A simulation model constructed with Aspen Plus was fitted to the binary and tertiary systems. The systems are described with the electrolyte non-random two liquid model (eNRTL) and predicts data of vapour pressures, physical solubility of CO_2, equilibrium constants, densities, and partial and total pressures of CO_2 in a good agreement with experimental values. The model provides a more complete overview of the design of the absorption system.

2. Modelling

In the Aspen Plus database, DEEA can be found as component. However, its cation was not found in the database and was added. The components, DEEA and $DEEAH^+$, together with their interaction with water, carbon dioxide and ions need to be fitted. The experimental data used to fit and validate the developed model are listed in Table 1.

Firstly, the vapour pressure of DEEA was regressed with Aspen Plus using data from Hartono et al. [15] and for water using information from NIST (National Institute of Standards and Technology) [26] and Kim et al. [27]. New values are presented for the Antoine's equation for both pure components, DEEA and H_2O (Table 6). Then, the binary system DEEA-H_2O was regressed using experimental data [15] and new

Table 6
Constants for H_2O and DEEA Antoine's equation and Henry's physical solubility optimized in this work.

$ln\ P(Pa) = A + \frac{B}{C+T} + D\ T + E\ lnT + F\ T^G$

A	B	C	D	E	F	G	Component
71,3163	−7816.9	14.40	0.0043	−7.08	−3.14E-6	1.94	H_2O
22.2127	−5057.22	−5662	−0.00982	0	0	0	DEEA

$ln\ H^{\infty}_{CO_2}\ (Mpa) = A + \frac{B}{T} + C\ lnT + DT + \frac{E}{T^2}$

A	B	C	D	E
22	−2350.47	−0.4701	0.00363	−476975

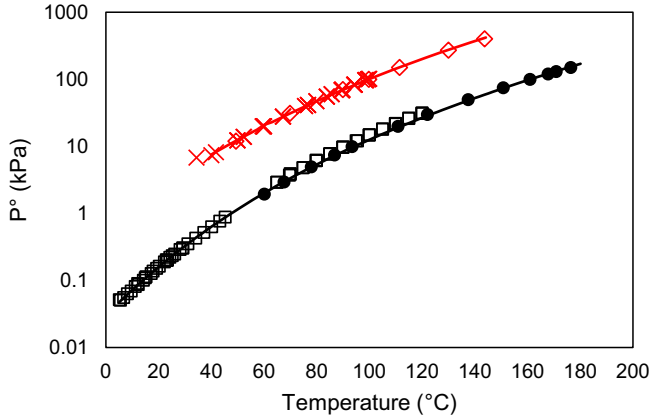

Fig. 1. Water and DEEA vapour pressures: this work (red and black lines, respectively); For H_2O, x from Kim et al. [27] and ◊ NIST [26]; For DEEA, + from Kapteina et al. [39] □ from Hartono et al. [15] • from Klepacova et al. [30].

interaction parameters were obtained. Additionally, the excess enthalpy was fitted using data from Mathonat et al. [23].

For loaded DEEA solutions, the partial pressure of CO_2 and total pressure data were used to fit physical solubility of CO_2 by regression. The new interaction parameters of the electrolyte pairs were obtained. Due to the high number of parameters to be fitted, the regression was improved with some final modifications by trial and error, using the CO_2 partial pressure and total pressure data [20,24] as outputs to be fitted.

Knowledge of densities is important for several applications within the absorption process: power required for pumping the unloaded and loaded solutions, influence in mass transfer, absorption rate and subsequently the efficiency of the entire process. The prediction of densities must be taken into account in order to obtain proper values in the calculation of the process. The densities of unloaded and loaded DEEA solutions were regressed in this work using the Racket model with Aspen Plus. New value for the Racket parameter (Z_{RA}) was obtained and results were validated with experimental data for DEEA-H_2O [25,28,29] and DEEA-H_2O-CO_2 systems [25].

In this work, the errors are reported by the parameter AARD, averaged absolute relative deviation (Eq. (1)).

$$AARD\ (\%) = \frac{1}{N}\sum_{i=k}^{N} 100\ \frac{|n_k - \varphi_k|}{\varphi_k} \tag{1}$$

The critical parameters as well as the acentric factor and compressibility factor are listed in Table 2.

The dielectric constant of DEEA was approximated to the value of trimethylamine due to the similarities in their structure. Values are included in Table 3, together with the values for H_2O.

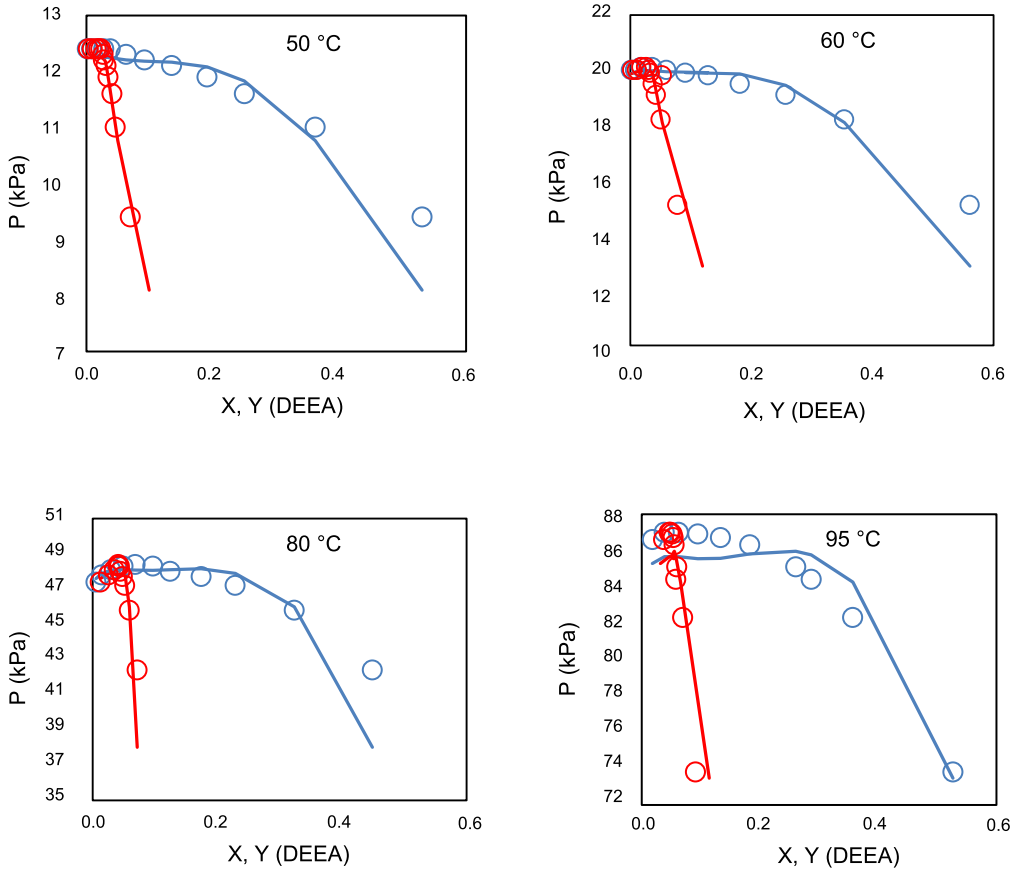

Fig. 2. VLE of DEEA-H_2O solutions at (from left to the right, from the top to the bottom) 50, 60, 80 and 95 °C: open points, experimental data from Hartono et al. [15]; solid lines, outputs from the Aspen model included in this work: red for the liquid phase and blue for the gas phase.

2.1. Vapour–liquid equilibrium

Tertiary amines do not react directly with CO_2 although they promote the hydrolysis process [33,34]. Tertiary amines react with CO_2 only at pH > 13 forming alkalycarbonates. The reactions (R1)–(R4) were considered in this work for the absorption of CO_2 in aqueous DEEA solutions.

$$2H_2O \leftrightarrow H_3O^+ + OH^- \quad \text{(R1)}$$

$$2H_2O + CO_2 \leftrightarrow H_3O^+ + HCO_3^- \quad \text{(R2)}$$

$$H_2O + HCO_3^- \leftrightarrow H_3O^+CO_3^{2-} \quad \text{(R3)}$$

$$DEEAH^+ + H_2O \leftrightarrow DEEA + H_3O^+ \quad \text{(R4)}$$

Chemical equilibrium is reached by the minimization of Gibbs free energy in the liquid phase [35]. The Redlich–Kwong equation was used for the fugacity in the vapour-phase. The activity coefficients for the species were derived from the excess Gibbs energy Eq. (2)

$$ln\gamma_i = \left[\frac{\delta(n_t * g^{ex*}/RT)}{\delta n_i}\right]_{T,P,nj\neq i} \quad (2)$$

Here n_t is total moles; g^{ex*} is the excess Gibbs energy of an electrolyte in solution and γ is the activity coefficient.

The CO_2 equilibria between liquid and gas phases is described in Eq. (3)

$$Y_i P \Phi i = X_i\, \gamma_i H_i^{\infty} exp\left[\frac{v_i^{\infty}(P - P^0)}{RT}\right] \quad (3)$$

Here, X_i and Y_i are the concentrations in the liquid and the vapour phases; γi are the activity coefficients of the species; Φ_i is the fugacity coefficient; P^0 is the saturated vapour pressure of the component; and v_i^{∞} and H_i^{∞} are the partial volume and Henry's law constant at infinite dilution of CO_2 in water at the system temperature. In this work, the Henry's coefficients for CO_2 were regressed with experimental VLE of the system DEEA-H_2O-CO_2 [20,24]. The fugacity is calculated based on the Gibbs energy or activity.

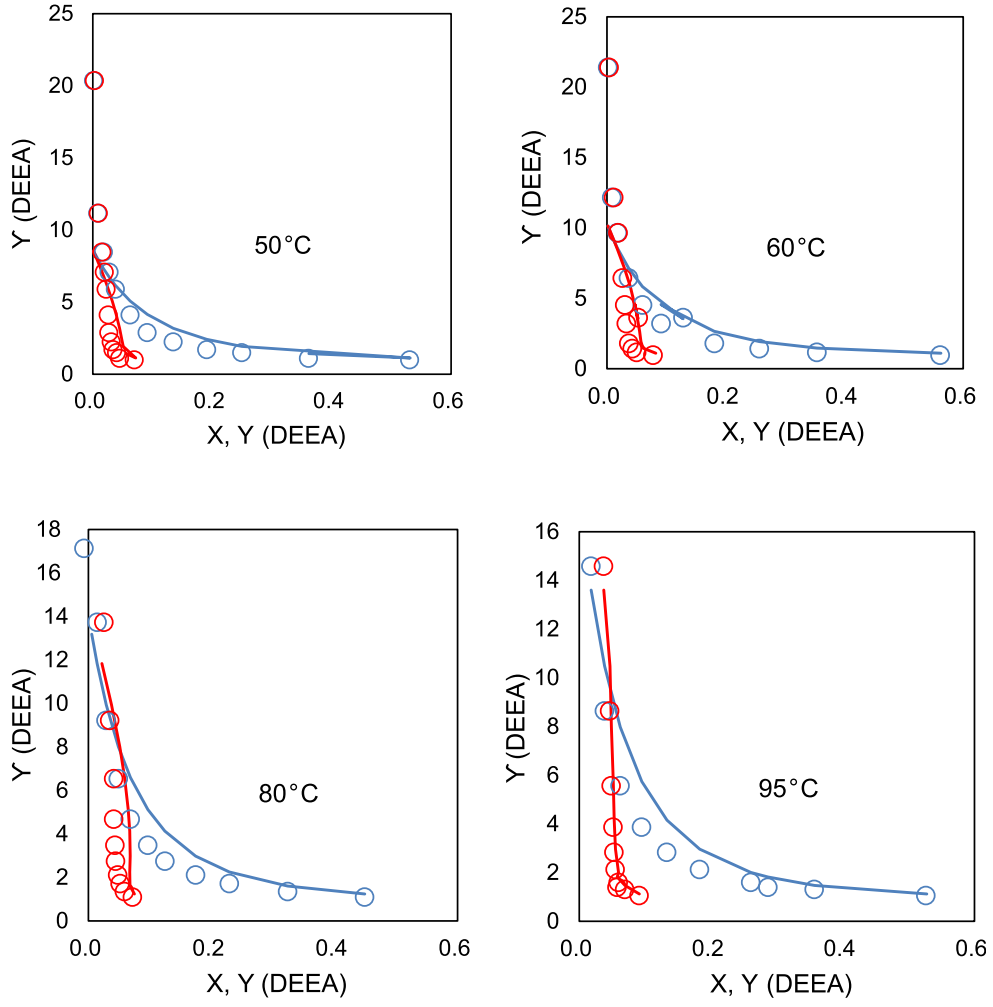

Fig. 3. Activity coefficients of DEEA and water at (from left to right, from the top to the bottom) 50, 60, 80 and 95 °C: open points from [15]; solid lines from this work: red for the liquid phase and blue for the gas phase.

All the equilibrium constants (molar fraction basis) used in this simulation model are included in Table 4. As seen from the table, the equilibrium constants of reactions (R1), (R2) and (R3) were taken from literature and only the equilibrium constant of reaction (R4) was fitted. Values for the equilibrium constant of reaction (R4) can be found in literature [20,21]. However, when using them in Aspen Plus the simulation results did not match the experimental data. Since small changes in these constants highly impacts the concentrations of the species in the gas and liquid phases, the equilibrium constant of reaction (R4) was fitted to be able to reproduce the experimental data.

2.2. Activity coefficient model

The eNRTL model was described 30 years ago [37]. It is used for the representation of the excess Gibbs energy and activity coefficients for electrolyte systems and assumes local electroneutrality and zero cation–cation repulsions. In this hypothesis, the ionic species are considered in the mixed solvent. In order to change from the infinite dilution in the mixed solvent to the aqueous phase, the Born term is defined as in Table 5 [35].

The electrolyte NRTL parameters relate the activity coefficient with the Gibbs free energy. It consists of both the non-randomness factors (α) and energy parameters (τ).

Table 7
eNRTL parameters.

Molecular parameters: $a_{m,m'}$, $b_{m,m'}$, $e_{m,m'}$					
$a_{H_2O,DEEA}$	4.34228	$b_{H_2O,DEEA}$	−763.917	$e_{H_2O,DEEA}$	0.619047
a_{DEEA,H_2O}	313.709	b_{DEEA,H_2O}	−152126	e_{DEEA,H_2O}	−45.3131
a_{H_2O,CO_2}	0[a]	b_{H_2O,CO_2}	0[a]	e_{H_2O,CO_2}	0[a]
a_{CO_2,H_2O}	0[a]	b_{CO_2,H_2O}	0[a]	e_{CO_2,H_2O}	0[a]
$a_{CO_2,DEEA}$	0[a]	$b_{CO_2,DEEA}$	0[a]	$e_{CO_2,DEEA}$	0[a]

Molecule/salt parameters: $a_{m,c/a}$, $b_{m,c/a}$			
$a_{H_2O,\ H_3O^+/OH^-}$	0	$b_{H_2O,H_3O^+/OH^-}$	0[a]
$a_{H_2O,H_3O^+/HCO_3^-}$	8[a]	$b_{H_2O,H_3O^+/HCO_3^-}$	0[a]
$a_{H_2O,H_3O^+/CO_3^{2-}}$	8[a]	$b_{H_2O,H_3O^+/CO_3^{-2}}$	0[a]
$a_{CO_2,H_3O^+/OH^-}$	15[a]	$b_{CO_2,H_3O^+/OH^-}$	0[a]
$a_{DEEA,H_3O^+/OH^-}$	0[a]	$b_{DEEA,H_3O^+/OH^-}$	0
$a_{H_2O,DEEAH^+/HCO_3^-}$	−4.0053	$b_{H_2O,DEEAH^+/HCO_3^-}$	311.364[b]
$a_{H_2O,DEEAH^+/OH^-}$	0	$b_{H_2O,DEEAH^+/OH^-}$	0
$a_{H_2O,DEEAH^+/CO_3^{-2}}$	−60	$b_{H_2O,DEEAH^+/CO_3^{-2}}$	−93.261[b]
$a_{CO_2,H_3O^+/CO_3^{-2}}$	15[a]	$b_{CO_2,H_3O^+/CO_3^{-2}}$	0[a]
$a_{CO_2,H_3O^+/HCO_3^-}$	15[a]	$b_{CO_2,H_3O^+/HCO_3^-}$	0[a]
$a_{CO_2,DEEAH^+/OH^-}$	−0.24226	$b_{CO_2,DEEAH^+/OH^-}$	−0.24226
$a_{CO_2,DEEAH^+/HCO_3^-}$	8.384[b]	$b_{CO_2,DEEAH^+/HCO_3^-}$	608.436[b]
$a_{CO_2,DEEAH^+/CO_3^{-2}}$	−2.7114[b]	$b_{CO_2,DEEAH^+/CO_3^{-2}}$	−527.063[b]
$a_{DEEA,H_3O^+/HCO_3^-}$	3.5081[b]	$b_{DEEA,H_3O^+/HCO_3^-}$	−602.792[b]
$a_{DEEA,H_3O^+/CO_3^{-2}}$	3.1376[b]	$b_{DEEA,H_3O^+/CO_3^{-2}}$	−282.638[b]
$a_{DEEA,DEEAH^+/OH^-}$	0	$b_{DEEA,DEEAH^+/OH^-}$	0
$a_{DEEA,DEEAH^+/HCO_3^-}$	9	$b_{DEEA,DEEAH^+/HCO_3^-}$	−810.104
$a_{DEEA,DEEAH^+/CO_3^{-2}}$	8.3565[b]	$b_{DEEA,DEEAH^+/CO_3^{-2}}$	−767.262[b]

Salt–molecules parameters: $a_{c/a,m}$, $b_{c/a,m}$			
$a_{H_3O^+/HCO_3^-,H_2O}$	−4[a]	$b_{H_3O^+/HCO_3^-,H_2O}$	0[a]
$a_{H_3O^+/CO_3^{2-},H_2O}$	−4[a]	$b_{H_3O^+/CO_3^{2-},H_2O}$	0[a]
$a_{H_3O^+/OH^-,CO_2}$	−8[a]	$b_{H_3O^+/OH^-,CO_2}$	0[a]
$a_{H_3O^+/OH^-,DEEA}$	−0.5	$b_{H_3O^+/OH^-,DEEA}$	0
$a_{DEEAH^+/HCO_3^-,H_2O}$	1.1823	$b_{DEEAH^+/HCO_3^-,H_2O}$	46
$a_{DEEAH^+/HCO_3^-,DEEA}$	2.5	$b_{DEEAH^+/HCO_3^-,DEEA}$	−126.497[b]
$a_{DEEAH^+/OH^-,DEEA}$	0	$b_{DEEAH^+/OH^-,DEEA}$	0
$a_{H_3O^+/HCO_3^-,CO_2}$	−8[a]	$b_{H_3O^+/HCO_3^-,CO_2}$	0[a]
$a_{H_3O^+/HCO_3^-,DEEA}$	−1.3105[b]	$b_{H_3O^+/HCO_3^-,DEEA}$	146.617[b]
$a_{H_3O^+/CO_3^{2-},CO_2}$	−8[a]	$b_{H_3O^+/CO_3^{2-},CO_2}$	0[a]
$a_{H_3O^+/CO_3^{2-},DEEA}$	−2.3338[b]	$b_{H_3O^+/CO_3^{2-},DEEA}$	151.66
$a_{DEEAH^+/OH^-,H_2O}$	0	$b_{DEEAH^+/OH^-,H_2O}$	0
$a_{DEEAH^+/OH^-,CO_2}$	−4.24226	$b_{DEEAH^+/OH^-,CO_2}$	−0.24226
$a_{DEEAH^+/HCO_3^-,CO_2}$	−6.6385	$b_{DEEAH^+/HCO_3^-,CO_2}$	200.853[b]
$a_{DEEAH^+/CO_3^{2-},H_2O}$	−4.4225[b]	$b_{DEEAH^+/CO_3^{2-},H_2O}$	−162
$a_{DEEAH^+/CO_3^{2-},CO_2}$	1.8621[b]	$b_{DEEAH^+/CO_3^{2-},CO_2}$	−53.014[b]
$a_{DEEAH^+/CO_3^{2-},DEEA}$	15.3149	$b_{DEEAH^+/CO_3^{2-},DEEA}$	−969.983[b]
$a_{H_3O^+/OH^-,H_2O}$	0	$b_{H_3O^+/OH^-,H_2O}$	0[a]

[a] Aspen default value.
[b] Monteiro et al. [20].

In this work, the molecule–molecule NRTL parameters have been optimized in the binary and tertiary systems. The interaction parameters for molecule–ion pairs and ion-pairs molecule were included in the modelling and fitted with the rest of parameters to reproduce the experimental data.

2.3. Density

The experimental data for the density of the binary system were regressed to the Racket model, which was chosen since it showed the best results in comparison to other models that Aspen incorporates in its database. Originally, this model correlates reduced properties with the compressibility factor. Aspen Plus incorporates the Racket model based on the modifications done later to this model [38]. The model equations are given below:

$$\frac{1}{\rho_s} = \frac{RT_c}{\rho_c} Z_{RA}^{(1+(1-T_r))^{2/7}} \tag{4}$$

$$T_c = \sum_i \sum_j x_i x_j V_{ci} V_{cj} \left(T_{ci} T_{cj}\right)^{1/2} \frac{1-k_{ij}}{V_{cm}^2} \tag{5}$$

$$\frac{T_c}{P_c} = \sum_i x_i \frac{T_{ci}}{P_{ci}} \tag{6}$$

$$Z_m^{RA} = \sum_i x_i Z_i^{RA} \tag{7}$$

$$V_{cm} = \sum_i x_i V_{ci} \tag{8}$$

$$T_r = \frac{T}{T_c} \tag{9}$$

$$k_{ij} = \frac{8\left(V_{ci} V_{cj}\right)^{1/2}}{\left(V_{ci}^{1/3} + V_{cj}^{1/3}\right)^3} \tag{10}$$

In the Equations (4)–(10), V_c, T_c are the critical volume and temperature; Z_{RA} is a specific constant for the Racket model; and x is the molar fraction.

3. Results

3.1. The pure systems: H_2O, DEEA

The default constant in Antoine's equation available in the Aspen Plus gave somewhat high deviations at temperatures above 100 °C. Thus, the constants in Antoine's equation were fitted using data covering the temperature ranges of 34–144 °C and 5–176.5 °C for water and DEEA, respectively. The optimised constants are given in Table 6 for both water and DEEA.

The simulation results, together with experimental data, are shown in Fig. 1. Generally, it can be said that the models represent the experimental data very well. For water, the AARD is 1.73%. For DEEA, the AARD is 1.9%, when data from Hartono et al. [15] are excluded and only data from and Kapteina et al. [39] and Klepacova et al. [30] are used in the fitting. As seen in the Fig. 1, the data from Hartono et al. [15] show slightly higher vapour pressures of DEEA in comparison to the other references and the model (AARD 13.7%).

3.2. Binary system: H_2O-DEEA

The molecule–molecule interaction parameters, τ_{ij}, for DEEA-H_2O were regressed together with the non-randomness parameters, using experimental data [20,24]. As seen in Fig. 2, the model produces results in a good agreement with the equilibrium of the binary system. The blue solid line is the total pressure of the solution plotted against the mole fraction of DEEA in the liquid phase (bubble point curve). The orange line is the total pressure of the solution as a function of the vapour phase concentration of DEEA (dew point). The total pressure and gas phase DEEA composition were calculated as a function of the fixed molar concentrations in the liquid phase, obtaining AARD of 1.76% and 11.79%, for the bubble point and DEEA concentration in the gas phase, respectively. As seen in the Fig. 2, the model is less accurate at very low DEEA concentrations and high temperature.

The activity coefficients are represented with AARD of 14.9% and shown in Fig. 3. As seen in Fig. 3, the activity coefficient decreases as the DEEA content increases. The regressed interaction parameters are given in Table 7.

In terms of the mixture of two pure liquids, in that case H_2O and DEEA, the excess of enthalpy is the change of isothermal enthalpy per mole of solution, which is similar to the heat of mixing of the solution. This property is significant because it is related to the excess Gibbs energy (Eq. (11)), which depends on the temperature. In the case of the eNRTL model, the excess of enthalpy (Eq. (12)) is dependent on the calculated interaction parameters, energy parameters (τ) and non-randomness factors (α) as seen from Equation (12). Consequently, the excess of enthalpy will impact the calculation of the VLE [27].

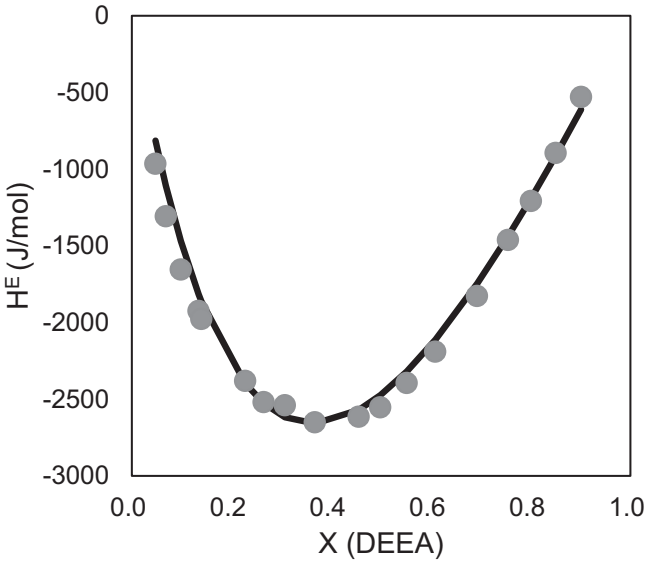

Fig. 4. Excess of enthalpy as function of composition at 298.15 K. Line represents the result from the simulation model from this work while points are from Mathonat et al. [23].

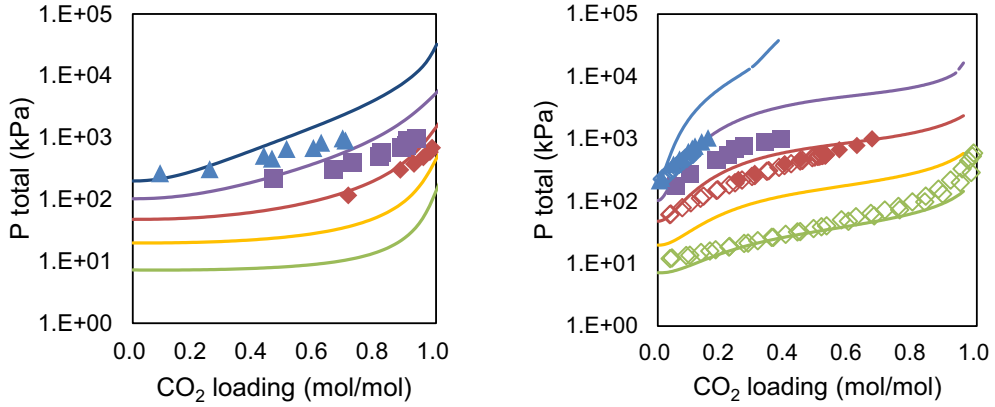

Fig. 5. Total pressure at 2 M (left) and 5 M (right). Filled points, experimental data from Monteiro et al. [20], open points, experimental data from Arshad et al. [24], solid lines, model predictions from this work. Colours: 40 °C (green), 60 °C (yellow), 80 °C (red), 100 °C (purple), 120 °C (blue).

$$\frac{d\frac{g_{ex}}{RT}}{d\left(\frac{1}{T}\right)} = \frac{-h_{ex}}{R} \tag{11}$$

$$\frac{-h_{ex}}{R} = \frac{x_1 x_2 b_{21} G_{21}(x_1(\alpha\tau_{21}-1)-x_2 G_{21})}{(x_1+x_2 G_{21})^2} + \frac{x_1 x_2 b_{12} G_{12}(x_2(\alpha\tau_{12}-1)-x_1 G_{12})}{(x_2+x_1 G_{12})^2} \tag{12}$$

The excess of enthalpy of the binary system DEEA-H_2O was considered in this work and is included in Fig. 4. It was analysed and compared with data from literature [23]. As seen in the Fig. 4, the model compares well with the experimental data, obtaining an AARD of 5.63%. It follows a parabolic shape with minimum at 0.4 molar fraction of DEEA. It means that it is an exothermic system with the highest release of heat of mixing at that point.

3.3. Tertiary system: H_2O-DEEA-CO_2

The loaded aqueous DEEA solutions were modelled as a reactive system (eNRTL model). The non-randomness parameters for CO_2, DEEA and H_2O were optimized, fixing the binary parameters as the values previously obtained. The eNRTL parameters were also modified and fitted to the experimental VLE data [20,24]. Moreover, the Henry constant, which represents the physical solubility of CO_2 at infinite dilution in water, was also refitted, because the values reported previously [15,20] were not in agreement with experimental results when used in the Aspen Plus environment. The values obtained are included in Tables 6 and 7.

As observed in Figs. 5 and 6, the partial pressure of CO_2 and total pressure of the system DEEA-H_2O-CO_2 increases as the loadings and/or temperature increase. At the lowest values of CO_2 loading, the slope of the curve (partial pressure against CO_2 loading) is high. There, a small change in the loading gives a high change in the partial pressure of CO_2. In this area, analytical and experimental inaccuracies have a large impact on the fit. This is the reason for discarding values of loadings below 0.041, as was done previously [20] (see Fig. 6).

As seen in Fig. 6, the experimental partial pressure of CO_2 and total pressures at high temperature, 100 and 120 °C, change the shape of the curve along the CO_2 loading. This shaping is not obvious with partial pressures of 5 M DEEA solutions. It has been observed that this model does not reproduce so well this change of trend. We speculate that this is due to the quality of experimental data or problems with model fitting. A possible hypothesis is the experimental results, since it is difficult to measure the low CO_2 partial pressures at high temperatures due to the high water pressure. Furthermore, sampling at

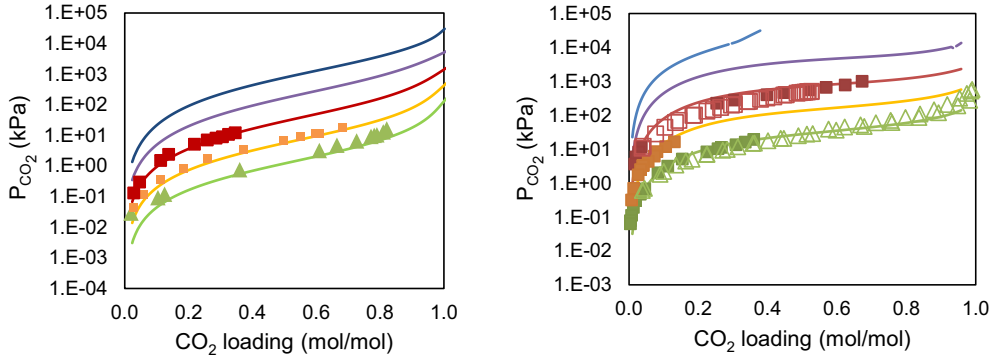

Fig. 6. CO_2 partial pressure at 2 M (left) and 5 M (right): Filled points, experimental data from Monteiro et al. [20], open points, experimental data from Arshad et al. [24], solid lines, model predictions from this work. Colours: 40 °C (green), 60 °C (yellow), 80 °C (red), 100 °C (purple), 120 °C (blue).

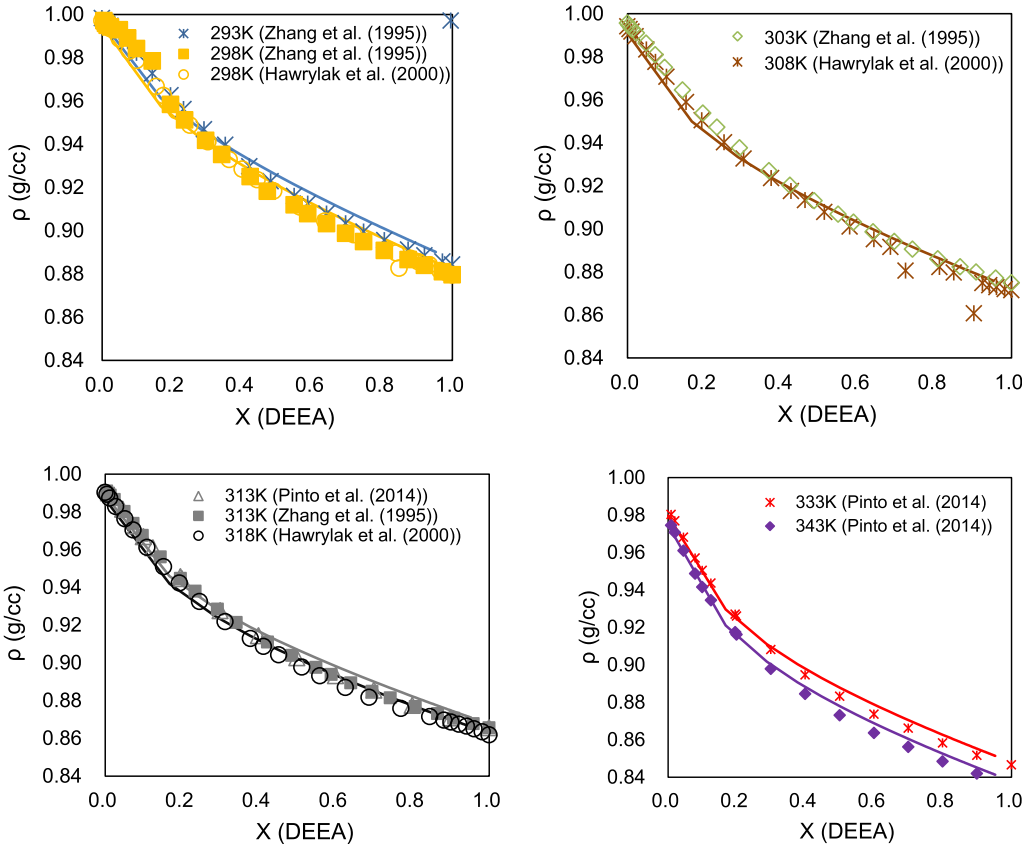

Fig. 7. Densities of DEEA solutions. Lines represent the simulation results from this work while points are experimental values from Zhang et al. [29], Hawrylak et al. [28] and Pinto et al. [25]. Colours: Top Left, blue (293 K) and yellow (298 K); Top right, green (303 K) and brown (308 K); Bottom, left, grey (313 K) and black (318 K); Bottom, right, red (333 K) and purple (343 K).

high temperatures can be a challenge. Thus, experimental CO_2 pressure data at high temperatures are often based on assumptions and "soft modelling". This hypothesis is supported by the differences between the experimental data of partial pressures at 120 °C from Monteiro et al. [20] and Arshad et al. [24] while the total pressure agree to each other.

The present model represents the experimental data on partial pressure of CO_2 with AARD of 19.45% while total pressure shows a AARD of 16.18%, at 40, 60 and 80 °C.

3.4. Density of the binary DEEA-H_2O and tertiary DEEA-CO_2-H_2O system

The experimental data for the density of the binary system were regressed to the Racket model (Eqs. (4−10)), which was chosen since it showed the best results in comparison to other models that Aspen Plus incorporates in its database.

The Racket parameter Z_{RA} (see Eqs. (4) and (7)) was regressed to 0.264187 using the experimental data from Pinto et al. [25]. The experimental results [25] were used to validate the densities of loaded DEEA solutions obtained with the model. The AARD is 1.38% and 1.66% for unloaded and loaded solutions respectively. As observed in Fig. 7, the density of unloaded solutions decreases as temperature and DEEA content increases. The density of loaded solutions increases as CO_2 loading increases in loaded solutions (Figs. (8) and (9)). For the binary system, there is a slight over-prediction at low DEEA content and under-prediction at high DEEA concentration, reproducing the same behaviour at the different temperatures studied.

For the tertiary system, although there is some over-prediction at low loadings and under-prediction at high loadings, the model agrees fairly well with experimental data. For loaded 61 wt% DEEA solutions, AARD is 1.49% (Fig. (8)) while it is 1.83% for 24 wt% DEEA solutions (Fig. (9)). The deviation increases at high loadings. Similar behaviour has been reported in the work of Pinto et al. [25], who observed a better fit at higher DEEA content in comparison to lower DEEA concentrations. The trend of the deviations is similar at all temperatures studied. The deviations are comparable with the modelling work from Pinto et al. [25] (Table 8), where the Racket, Redlich-Kister and a proposed proportional model were studied. In their work, a better fit was obtained using the Redlich-Kister and proportional models in comparison to the Racket model. In the present work, the representation of densities of loaded systems using the Racket model has been improved by 17.54%, from the AARD of 19.2% shown in Pinto et al. [25] to 1.66% in this work. For unloaded systems, there is a small difference of 0.455% AARD, higher in this work compared to Pinto et al. [25].

4. Summary

In this work, a model was developed in Aspen Plus to describe the system DEEA-H_2O-CO_2. This model reproduces the experimental VLE, excess of enthalpy and density data.

Table 8 includes a comparison of all the simulation results obtained in this work to previously published in-house models [20,24,25]. We can see that the developed model is able to predict the CO_2 partial pressure. However, the total pressure is not predicted as well, which is partly due to the inconsistent data in the literature. Whereas the previous models only used their data at high temperatures, in this work all available data was used. The assumptions made to calculate partial pressures from the experimental total pressure data at high temperatures involve assumptions about idealities that might not be correct. The model reproduces the excess of enthalpy data of the binary system DEEA-H_2O well. The prediction of the density using the Racket model strongly agrees with experimental results, showing a considerable improvement in the binary system DEEA-H_2O compared to previous reported values.

5. Conclusions

To design the absorption and desorption columns through the use of simulation models, the behaviour of the chemical system must be simulated accurately. In the case of CO_2 absorption, the most important predictions are the solubility of CO_2 and kinetics of the CO_2 absorption, together with physical properties like the density and viscosity of the solvent [40].

In this work, a simulation model based on the eNRTL theory was created in Aspen Plus. New parameters for the Antoine's equation were presented with DEEA and H_2O, with an AARD of 1.9% and 1.73% respectively. New interaction parameters were obtained for the binary and tertiary system. The heat of mixing of the binary system H_2O-DEEA showed a AARD of 5.63% and the total pressure has an AARD of 1.76%.

For the tertiary system DEEA-H_2O-CO_2, the model represented the partial pressures with an AARD of 19.45% while it was 16.48% for the total pressures. Temperatures higher than 80 °C were not used for fitting due to differences in the available experimental data, although the data were included in the graphs.

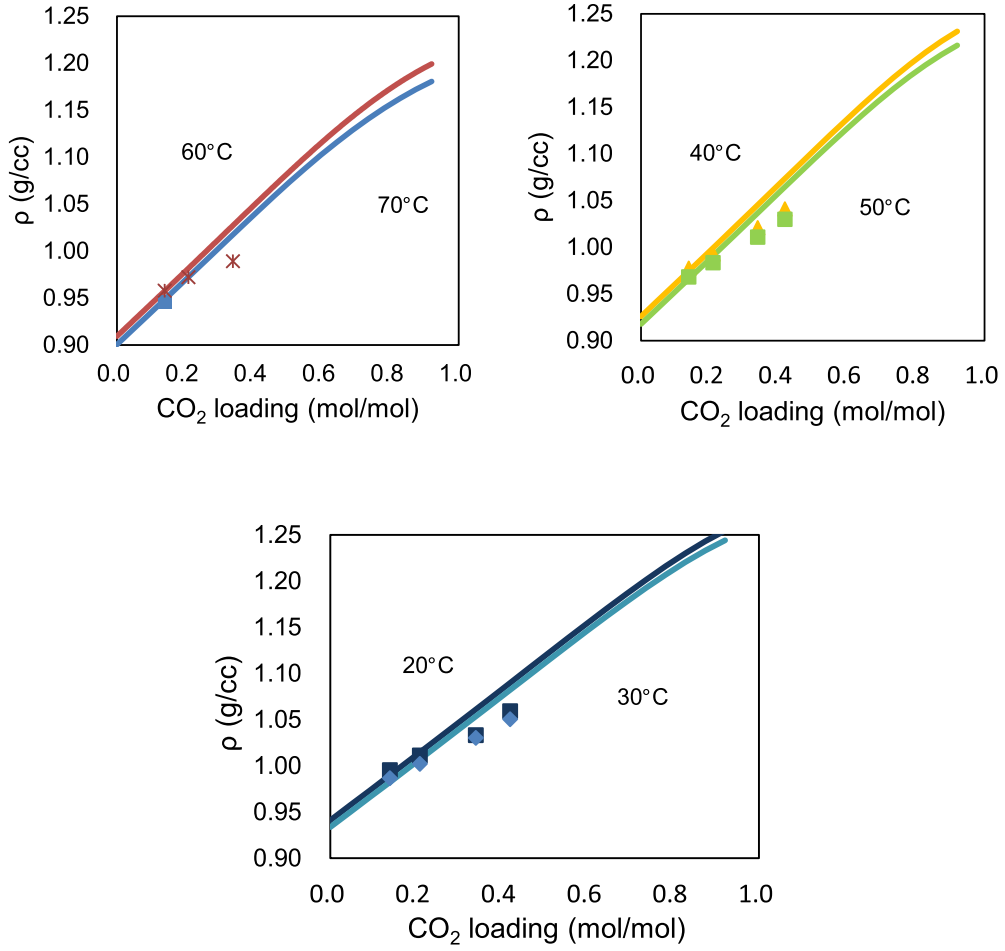

Fig. 8. Densities of loaded 61 wt% DEEA solutions from 293 to 313 K: Experimental values from Pinto et al. [25] (points) and simulation values (lines) from this work.

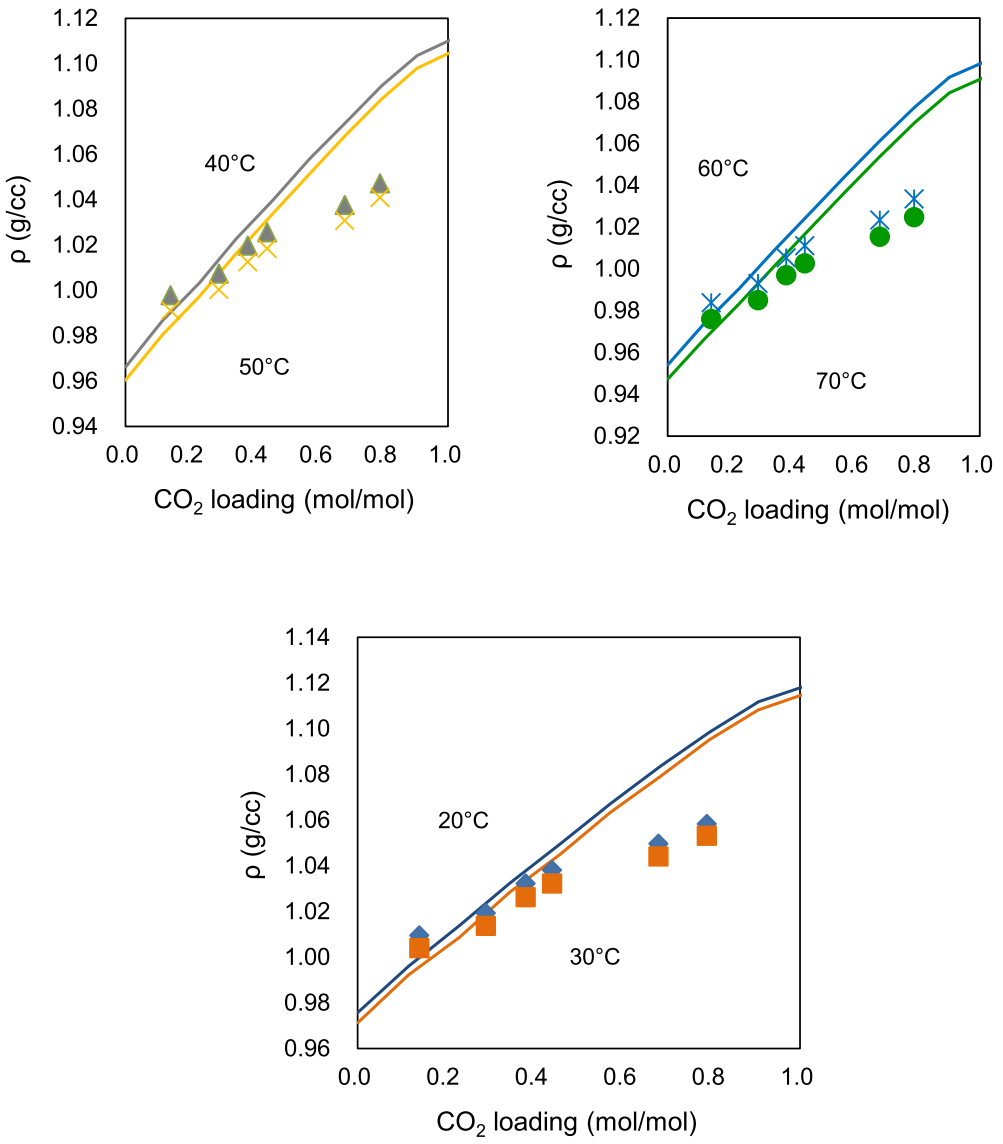

Fig. 9. Densities of loaded 24 wt% DEEA solutions from 293 to 313 K. Experimental values (points) from Pinto et al. [25] and simulation values (lines) from this work.

Table 8
% AARD obtained in this work in comparison to modelling works reported in the literature.

Parameter	%AARD	Source	%AARD (This work)
Total pressure DEEA-H_2O	1 0.7	[15] [20]	1.76
Partial Pressure of the system DEEA-H_2O-CO_2	15.5 19.1	[20] [24]	19.45
Total Pressure of the system DEEA-H_2O-CO_2	8.1 11	[20] [24]	16.18
Density (Racket model) of the system DEEA-H_2O	19.2	[25]	1.66
Density (Racket model) of the system DEEA-H_2O-CO_2	0.925	[25]	1.38
Excess of enthalpy in the binary system DEEA-H_2O	3.8 7.2	[20] [24]	5.63

The model was also valid for the simulation of the densities of unloaded and loaded DEEA solutions, using the Racket model. The Racket parameter was regressed, which obtained an AARD of 1.38% for aqueous DEEA solutions and 1.66% for loaded solutions.

Overall, this single model constructed with Aspen Plus represents the density and VLE for the pure (H_2O, DEEA), binary (H_2O-DEEA) and tertiary (CO_2-H_2O-DEEA) systems in a good agreement with experimental data. Moreover, the model reproduces the experimental excess of enthalpy of the binary system. Compared to previous models, this model provides a good prediction of the density and the VLE of pure, binary and tertiary systems.

Conflict of interest

The authors declare that there is no conflict of interest in the subject matter or materials discussed in this manuscript.

Acknowledgments

The authors would like to acknowledge the financial support of the EPSRC grant EP/J020184/1 and the UK CCS Research Centre (www.ukccsrc.ac.uk) in carrying out this work. The UKCCSRC is funded by the EPSRC as part of the RCUK Energy Programme (EP/K000446/1).

References

[1] P.D. Vaidya, E.Y. Kenig, CO_2 capture by novel amine blends, Advances in Gas Processing. 1, 2009, pp. 239–246.
[2] I. Kim, H.F. Svendsen, Int. J. Greenh. Gas. Control 5 (3) (2011) 390–395.
[3] D. Byles, M.P. Conservative, N. Warwickshire, B. Gardiner, M.P. Labour, B. North, I. Lavery, House of commons energy and climate change committee. The future of marine renewables in the UK (II), 2012.
[4] European Commission, Eur. Comm. (2014).
[5] M. Gupta, E.F. Da Silva, H.F. Svendsen, Energy Proc. 51 (1876) (2014) 161–168.
[6] I. von Harbou, H.P. Mangalapally, H. Hasse, Int. J. Greenh. Gas. Control 18 (2013) 305–314.
[7] H.P. Mangalapally, R. Notz, S. Hoch, N. Asprion, G. Sieder, H. Garcia, H. Hasse, Energy Proc. 1 (1) (2009) 963–970.
[8] Y. Artanto, J. Jansen, P. Pearson, T. Do, A. Cottrell, E. Meuleman, P. Feron, Fuel 101 (2012) 264–275.
[9] W. Conway, Y. Beyad, P. Feron, G. Richner, G. Puxty, Energy Proc. 63 (2014) 1835–1841.
[10] C. Chen, Z. Xu, S. Wang, J. Combust. Sci. Technol. 19 (2) (2013) 103–108.
[11] U. Liebenthal, D.D.D. Pinto, J.G.M.-S. Monteiro, H.F. Svendsen, A. Kather, Energy Proc. 37 (2013) 1844–1854.
[12] P.C. Chen, C.C. Liao, 3 (4) (2014) 78–82.
[13] P.B. Konduru, P.D. Vaidya, E.Y. Kenig, Activated DEEA process for CO_2 capture, Advances in Gas Processing, 2010, pp. 21–29.
[14] H. Kierzkowska-Pawlak, Int. J. Greenh. Gas. Control 37 (2015) 76–84.
[15] A. Hartono, F. Saleem, M. Waseem Arshad, M. Usman, H.F. Svendsen, Chem. Eng. Sci. 101 (2013) 401–411.
[16] M.W. Arshad, N. Von Solms, K. Thomsen, H.F. Svendsen, Energy Proc. 37 (1876) (2013) 1532–1542.
[17] P. Brœder, H.F. Svendsen, Energy Proc. 23 (1876) (2012) 45–54.
[18] W. Conway, S. Bruggink, Y. Beyad, W. Luo, I. Melián-Cabrera, G. Puxty, P. Feron, Chem. Eng. Sci. 126 (2015) 446–454.
[19] A. Kohl, R. Nielsen, Gas purification, fifth ed., 1997. Houston, Texas.
[20] J.G.M.S. Monteiro, D.D.D. Pinto, S.a H. Zaidy, A. Hartono, H.F. Svendsen, Int. J. Greenh. Gas. Control 19 (2013) 432–440.
[21] Z. Xu, S. Wang, G. Qi, A. a. Trollebø, H.F. Svendsen, C. Chen, Int. J. Greenh. Gas. Control 29 (2014) 92–103.
[22] H. Touhara, S. Okazaki, F. Okino, H. Tanaka, K. Ikari, K. Nakanishi, J. Chem. Thermodyn. 14 (1982) 145–156.
[23] C. Mathonat, Y. Maham, A.E. Mather, L.G. Hepler, J. Chem. Eng. Data 42 (96) (1997) 993–995.
[24] M. Waseem Arshad, K. Thomsen, N. von Solms, Measuring and thermodynamic modeling of de-mixing CO_2 capture systems, Technical University of Denmark, 2014.
[25] D.D.D. Pinto, J.G.M.-S. Monteiro, B. Johnsen, H.F. Svendsen, H. Knuutila, Int. J. Greenh. Gas. Control 25 (2014) 173–185.
[26] NIST chemistry webbook, National Institute of Standards and Technology (http://webbook.nist.gov/chemistry).
[27] I. Kim, H.F. Svendsen, E. Børresen, J. Chem. Eng. Data 53 (11) (2008) 2521–2531.
[28] B. Hawrylak, S.E. Burke, R. Palepu, J. Solut. Chem. 29 (6) (2000) 575–594.
[29] F. Zhang, H.-P. Li, M. Dai, J.-P. Zhao, J.P. Chao, Thermochim. Acta 254 (1995) 347–357.
[30] K. Klepáčová, P.J.G. Huttenhuis, P.W.J. Derks, G.F. Versteeg, J. Chem. Eng. Data 56 (2011) 2242–2248.
[31] C.L. Yaws, P.K. Narasimhan, Thermophys. Prop. Chem. Hydrocarb. (973) (2006) 1–95.
[32] CRC handbook of chemistry and physics. 86, CRC Press, IN., Boca Raton, FL, 2006.
[33] T.L. Donaldson, Y.N. Nguyen, Ind. Eng. Chem. Fundam. 19 (3) (1980) 260–266.
[34] G.F. Versteeg, W.P.M. van Swaaij, Chem. Eng. Sci. 43 (3) (1988) 587–591.
[35] D.M. Austgen, G.T. Rochelle, C.-C. Chen, Ind. Eng. Chem. Res. (1967) (1989) 1060–1073.
[36] T.J. Edwards, G. Maurer, J. Newman, J.M. Prausnitz, AIChE J. 24 (6) (1978) 966–976.
[37] C.-C. Chen, L.B. Evans, Alche J. 32 (3) (1986) 444–454.
[38] F. Calvin, R.P. Danner, J. Chem. Eng. Data 17 (2) (1972) 236–241.
[39] S. Kapteina, K. Slowik, S.P. Verevkin, A. Heintz, J. Chem. Eng. Data 50 (2) (2005) 398–402.
[40] S. Mokraoui, A. Valtz, C. Coquelet, D. Richon, Thermochim. Acta 440 (2) (2006) 122–128.